

Rabi model beyond the rotating wave approximation: generation of photons from vacuum through decoherence

T. Werlang,¹ A. V. Dodonov,¹ E. I. Duzzioni,² and C.J. Villas-Bôas¹

¹*Departamento de Física, Universidade Federal de São Carlos,
P.O. Box 676, São Carlos, 13565-905, São Paulo, Brazil*

²*Centro de Ciências Naturais e Humanas, Universidade Federal do ABC,
Rua Santa Adélia, 166, Santo André, São Paulo, 09210-170, Brazil*

We study numerically the dynamics of the Rabi Hamiltonian, describing the interaction of a single cavity mode and a two-level atom without the rotating wave approximation, subjected to damping and dephasing reservoirs included via usual Lindblad superoperators in the master equation. We show that the combination of the antirotating term and the atomic dephasing leads to linear asymptotic photons generation from vacuum. We reveal the origins of the phenomenon and estimate its importance in realistic situations.

PACS numbers: 42.50.-p,03.65.-w,42.50.Pq

I. INTRODUCTION

A fundamental task in Physics is the description of the matter-light interaction. The most simple model to deal with is the Rabi model [1], which describes the interaction of a two-level atom with a single mode of the quantized electromagnetic (EM) field. The Rabi Hamiltonian (RH) reads ($\hbar = 1$)

$$H = \omega a^\dagger a + \frac{\omega_0}{2} \sigma_z + g (\sigma_+ + \sigma_-) (a + a^\dagger), \quad (1)$$

where ω and ω_0 are the field and atomic transition frequencies, respectively, and g is the coupling constant (vacuum Rabi frequency). a (a^\dagger) is the annihilation (creation) operator of the EM field, $\sigma_z = |e\rangle\langle e| - |g\rangle\langle g|$ and $\sigma_+ = |e\rangle\langle g|$ ($\sigma_- = \sigma_+^\dagger$) are atomic operators, with $|g\rangle$ and $|e\rangle$ denoting the ground and excited atomic states, respectively. Although largely studied over the last decades, up to now its exact analytical solution is lacking and only numerical [2, 3, 4, 5] and approximate analytical solutions are available [6, 7, 8], despite the conjecture by Reik and Doucha [9] that an exact solution of RH in terms of known functions is possible. The most used analytical approach to RH is to make the rotate wave approximation (RWA), where the antirotating term $g (a^\dagger \sigma_+ + a \sigma_-)$ is neglected, since in the weak coupling regime $g/\omega \ll 1$, small detuning $|\Delta| \ll \omega$ ($\Delta = \omega_0 - \omega$), and weak field amplitude its contribution to the evolution of the system is quite small [10, 11]. In this limit the RH is known as Jaynes-Cummings Hamiltonian (JCH) [12, 13] and can be integrated exactly.

For having an exact solution, the JCH has been largely employed in Quantum Optics, in particular in cavity quantum electrodynamics (QED) [14, 15], where the vast majority of the experiments satisfy the required parameters regime [10, 11]. JCH revealed interesting phenomena related to the quantum nature of the light, encompassing the granular nature of the electromagnetic field, revealed through collapse and revivals of the atomic inversion [16], Rabi oscillations [17], squeezing [18], non-classical states,

such as Schrödinger cat state-like [19] and Fock states [20], and the entanglement between atom-atom or atom-field [21]. The manipulation of atom-field interaction has been employed in the implementation of quantum logic gates in trapped ions [22] and in cavity QED [23], as well as the atomic teleportation process [24], which have contributed for a fast development of the quantum information science [25]. Moreover, over the past few years the JCH was experimentally investigated in solid state cavity QED systems in the strong coupling regime using superconducting artificial two-level atoms coupled to microwave waveguide resonators [26, 27, 28] (the so called *circuit* QED [29]) and quantum dots coupled to photonic crystals microcavities [30, 31]. In fact, in circuit QED the JCH is the basic theoretical tool for describing quantum logic gates and read-out protocols [32, 33].

The antirotating term neglected under RWA is usually wrongly interpreted as being non-conservative [10, 11, 34], once it could allow for a violation of the energy conservation. In fact, this term does not conserve the *total number of quanta* of the system, defined by the operator $N \equiv a^\dagger a + \sigma_z + \mathbb{I}$ (where \mathbb{I} stands for identity operator). However, it does not change the *total energy* of the system, as can be easily seen through the Heisenberg equation of motion for the total Hamiltonian operator $dH/dt = i[H, H] + \partial H/\partial t = 0$, once H in Eq. (1) is time independent. Therefore, the total energy of the system $\langle H \rangle$ is conserved and no violation of physical laws occur. Besides, recent works questioned the validity of the RWA [35, 36, 37] and proposed alternative analytical approximate methods [6, 8]. Moreover, it was shown that the antirotating term is responsible for several novel quantum mechanical phenomena, such as quantum irreversibility and chaos [38, 39], quantum phase transitions [40], implementation of Landau-Zener transitions of a qubit in circuit QED architecture [41, 42], generation of atom-cavity entanglement [43, 44], and simulation of the dynamical Casimir effect (DCE [45]) in semiconducting microcavities [46, 47, 48] or circuit QED [44].

In this work we study numerically the dynamics of the

RH subjected to dissipative effects acting on both the atom and cavity mode. These undesirable effects are taken into account through the master equation approach [10], where the Lindblad superoperators are built *as usual* [49]. Without any formal prove, we simply assume that the evolution of the density operator of the system $\rho(t)$ is described by the master equation

$$\frac{\partial \rho}{\partial t} = -i[H, \rho] + \mathcal{L}(\rho), \quad (2)$$

where H is the RH (1) and the Lindblad operator $\mathcal{L}(\rho)$ is given by

$$\mathcal{L}(\rho) = \mathcal{L}_a(\rho) + \mathcal{L}_d(\rho) + \mathcal{L}_f(\rho), \quad (3)$$

with the standard definitions

$$\begin{aligned} \mathcal{L}_a(\rho) &= \frac{\gamma}{2}(n_t + 1)(2\sigma_- \rho \sigma_+ - \sigma_+ \sigma_- \rho - \rho \sigma_+ \sigma_-) \\ &+ \frac{\gamma}{2}n_t(2\sigma_+ \rho \sigma_- - \sigma_- \sigma_+ \rho - \rho \sigma_- \sigma_+), \end{aligned} \quad (4)$$

$$\begin{aligned} \mathcal{L}_f(\rho) &= \frac{\kappa}{2}(n_t + 1)(2a\rho a^\dagger - a^\dagger a \rho - \rho a^\dagger a) \\ &+ \frac{\kappa}{2}n_t(2a^\dagger \rho a - a a^\dagger \rho - \rho a a^\dagger), \end{aligned} \quad (5)$$

$$\mathcal{L}_d(\rho) = \gamma_{ph}(\sigma_z \rho \sigma_z - \rho). \quad (6)$$

The superoperators $\mathcal{L}_a(\rho)$ and $\mathcal{L}_f(\rho)$ describe the thermal reservoirs effects (with mean photon number n_t) on the atom and field, respectively, where γ (κ) is the atom (cavity) relaxation rate. Another source of decoherence of the atom is the phase damping reservoir, represented by $\mathcal{L}_d(\rho)$, where γ_{ph} is the dephasing rate. By focusing our attention on the asymptotic *photons creation from vacuum* driven by the combination of the antirotating term $g(a^\dagger \sigma_+ + a \sigma_-)$ in (1) and the atomic phase reservoir, we show that even in situations where the atom and field are initially prepared in their individual ground states, i.e., $|\phi\rangle = |g, 0\rangle$, where $|0\rangle$ is the ground state of the EM field, there is an asymptotic photons generation. This process depends on the intensity of the atom-field coupling g , the detuning Δ , and it is considerably amplified when the atomic phase reservoir is predominant over the other dissipative channels, such as atomic and field damping due to the thermal reservoirs. The essence of the photons creation mechanism presented here relies on the existence of the antirotating term in the RH and the limitation imposed by the quantum vacuum, namely, $a|0\rangle = 0$. The role played by the atomic phase reservoir is just to amplify the photons creation process through atomic decoherence. As far as we know, this phenomenon has not been described in the literature.

This work is organized as follows. In Sec. II we study in details the process of photons generation due to the atomic dephasing and explain its origin. In Sec. III we give an alternative physical explanation of photons generations by considering that the atom's dephasing is due to random shifts of the atomic transition frequency, as usually occurs in solid state systems (e.g. circuit QED).

In Sec. IV we study the influence of damping process on the photons creation through decoherence and estimate the net effect in realistic situations. Finally, the section V contains discussion of results and concluding remarks.

II. PURE DEPHASING

For convenience, from now on we set the cavity frequency to $\omega = 1$. First we integrated numerically the Eq. (2) considering just the dephasing reservoir ($\gamma = \kappa = 0$). In Figs. 1 and 2 we set the parameters $\Delta = 0$ and $g = 0.1$. These and other values of the parameters were chosen in order to optimize the numerical calculations, and are not related to the experimental data; nevertheless, we checked out that qualitatively the behavior described below also holds for realistic parameters (see Fig. 5b below). The state $|g, 0\rangle$ is the ground state of the JCH, so it is not coupled to other states under the JCH dynamics. On the other hand, the antirotating term in the RH does induce transitions to other states and, since the atom and field states are limited from below by $|g\rangle$ and $|0\rangle$, respectively, these transitions may only *increase* $\langle n \rangle$. In Fig. 1a we plot the mean photon number $\langle n \rangle$ without dephasing ($\gamma_{ph} = 0$, line 1) as function of the dimensionless time $\tau \equiv \xi t$ with $\xi = 0.1$ for the initial state $|g, 0\rangle$, showing a bound oscillating behavior as described in details in [3]. Fig. 1a also shows $\langle n \rangle$ (line 2) and the Mandel factor $q = (\langle \Delta n \rangle^2 - \langle n \rangle) / \langle n \rangle$ (line 3) for dephasing rate $\gamma_{ph} = 0.1$: now $\langle n \rangle$ increases with time, achieving asymptotically a linear behavior, and the generated field state demonstrates a super-poissonian behavior, $q > 0$.

The photons creation mechanism through atomic dephasing demonstrated in Fig. 1a is a general phenomenon and asymptotically does not depend on the initial state of the system. In Fig. 1b we plot $\langle n \rangle$ *versus* τ for 6 different initial states: $|\phi_1\rangle = |g, 0\rangle$, $|\phi_2\rangle = |g, \alpha\rangle$ where $|\alpha\rangle$ is the coherent state and we take $|\alpha|^2 = 0.05$, $|\phi_3\rangle = [(|g\rangle + |e\rangle) / \sqrt{2}] \otimes |0\rangle$, $|\phi_4\rangle = [(|g\rangle + |e\rangle) / \sqrt{2}] \otimes |\alpha\rangle$, $|\phi_5\rangle = |e, 0\rangle$, and $|\phi_6\rangle = |e, \alpha\rangle$. The basic difference between these initial states is the amount of quanta $\langle N_k \rangle = \langle \phi_k | N | \phi_k \rangle$: we have $\langle N_1 \rangle = 0$, $\langle N_2 \rangle = 0.05$, $\langle N_3 \rangle = 0.5$, $\langle N_4 \rangle = 0.55$, $\langle N_5 \rangle = 1$ and $\langle N_6 \rangle = 1.05$. We see that after the transient regime ($\tau \gtrsim 15$), which is proportional to the initial number of quanta, all curves present the same behavior – a linear time dependence with the same photons creation rate. In Fig. 1c we plot the atomic population inversion $\langle \sigma_z \rangle$ for these states, showing that asymptotically $\langle \sigma_z \rangle$ approaches zero for any initial state. This result was expected due to the atomic decoherence.

The master equation describes only the net effect of the environment on the system. For a better understanding of the role played by the atomic dephasing on the creation of photons we use the quantum trajectories approach [49, 50] to study $\langle n \rangle$ during individual trajectories. Here the quantum jump operator is $J\rho = \gamma_{ph} \sigma_z \rho \sigma_z$ and the non-

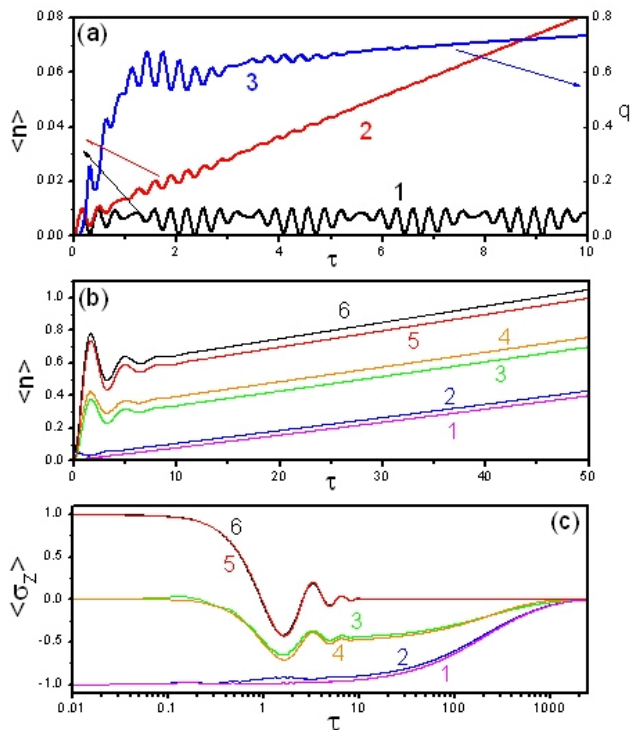


FIG. 1: Dynamics of the Rabi Hamiltonian for $\Delta = 0$ and $g = 0.1$ as function of dimensionless time $\tau = \xi t$ ($\xi = 0.1$). **a)** Mean photon number $\langle n \rangle$ for initial state $|g, 0\rangle$ without dephasing (line 1) and with dephasing $\gamma_{ph} = 0.1$ (line 2). There is photon generation from vacuum due to atomic dephasing and the created field state is superpoissonian, since the Mandel factor $q > 0$ (line 3). **b)** $\langle n \rangle$ for different initial states $|\phi_i\rangle$, $i = 1, \dots, 6$ (see the text), demonstrating that the asymptotic photons generation does not depend on the initial state. **c)** Population inversion $\langle \sigma_z \rangle$ for the states $|\phi_i\rangle$ shown in (b): as expected, $\langle \sigma_z \rangle$ goes to zero asymptotically due to the decoherence.

Hermitian Hamiltonian is $\tilde{H} = H - i(\gamma_{ph}/2)\mathbb{I}$. In Fig. 2 (a)-(c) we plot $\langle n \rangle$ versus τ for 3 samples of individual trajectories for the initial number state $|g, 5\rangle$, where we notice that in each trajectory $\langle n \rangle$ tends to increase as the time goes on. This occurs for two reasons: (i) the antirotating term in RH and (ii) the limitation of the cavity field from below by the vacuum, $a|0\rangle = 0$.

To illustrate (i) we plot in Fig. 2d $\langle n \rangle$ obtained via quantum trajectories approach for the JCH under the atomic dephasing, where we see that $\langle n \rangle$ oscillates with time but does not increase, contrary to the Figs. 2 (a)-(c). To explain the process of photon creation, we notice that any state may be written in terms of the basis states $\{|s, n\rangle\}$ (with $s = \{g, e\}$ and $|n\rangle$ the Fock state). Between the jumps, the system evolves according to the Rabi Hamiltonian (1) (the non-hermitian part is not important due to the normalization condition [51]) The JC term $[g(a\sigma_+ + a^\dagger\sigma_-)]$ promotes $|g, n\rangle \leftrightarrow |e, n-1\rangle$ transitions, while the antirotating term induces $|g, n\rangle \leftrightarrow |e, n+1\rangle$.

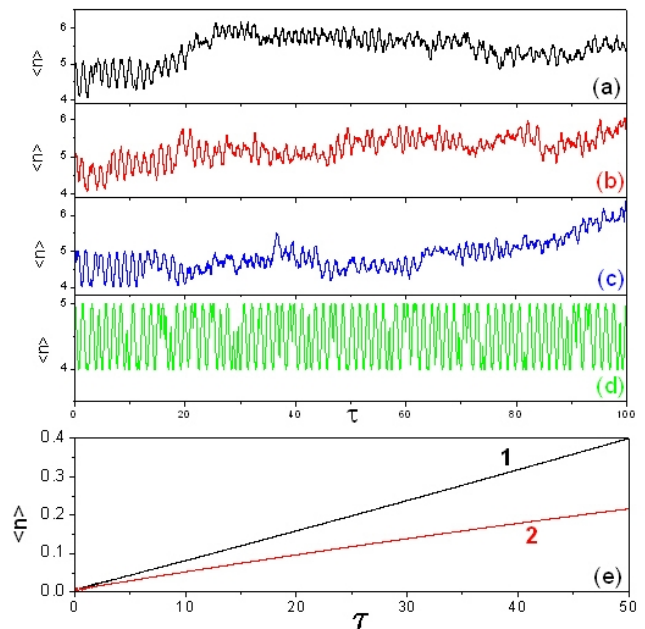


FIG. 2: **a-c)** Mean photon number for RH $\langle n \rangle$ versus τ for three particular trajectories, obtained using the quantum trajectories approach. The parameters are $\Delta = 0$, $g = 0.1$, $\gamma_{ph} = 0.1$ and the initial state is $|g, 5\rangle$. $\langle n \rangle$ tends to increase with time. **d)** $\langle n \rangle$ for a single trajectory using JCH, showing that there is no increase of the photon number without the antirotating terms. **e)** Asymptotic increase of mean photon number for the RH (line 1) and the test Hamiltonian H_E (line 2, see text), demonstrating that the phenomenon is due to the antirotating terms and the limitation by vacuum, $a|0\rangle = 0$.

The combined action of both parts generates all the possible transitions. However, the Fock states are limited from below by the vacuum state (ii), so there are more available states $|s, m > n\rangle$ than $|s, m < n\rangle$ and the mean number of photons between the jumps tends to increase. Upon a jump, the reservoir reads out the atom's state (through the application of σ_z on the wavefunction, which transforms $|g\rangle \rightarrow -\sqrt{\gamma_{ph}}|g\rangle$ and $|e\rangle \rightarrow \sqrt{\gamma_{ph}}|e\rangle$) so the coherence between the states $|g\rangle$ and $|e\rangle$ is lost and subsequent evolution under H will not bring the system to the state at the moment of the previous jump. For this reason after each jump $\langle n \rangle$ tends to be larger than upon the last jump, as clearly demonstrated in Figs. 2(a)-(c). After making a statistical average over many trajectories one finds out that $\langle n \rangle$ always increases, in agreement with Fig. 1.

One could suspect a third explanation for photons generation due to atomic dephasing – the different weights \sqrt{n} and $\sqrt{n+1}$ arising upon operating a and a^\dagger on the Fock state $|n\rangle$. To show that this is not the case we consider the test Hamiltonian H_E obtained through the substitution of the operators a and a^\dagger in RH (1) by the exponential phase operators [52, 53] $E_- \equiv (n+1)^{-1/2} a$ and $E_+ = E_-^\dagger$, respectively, where $E_+E_- = 1 - |0\rangle\langle 0|$. By

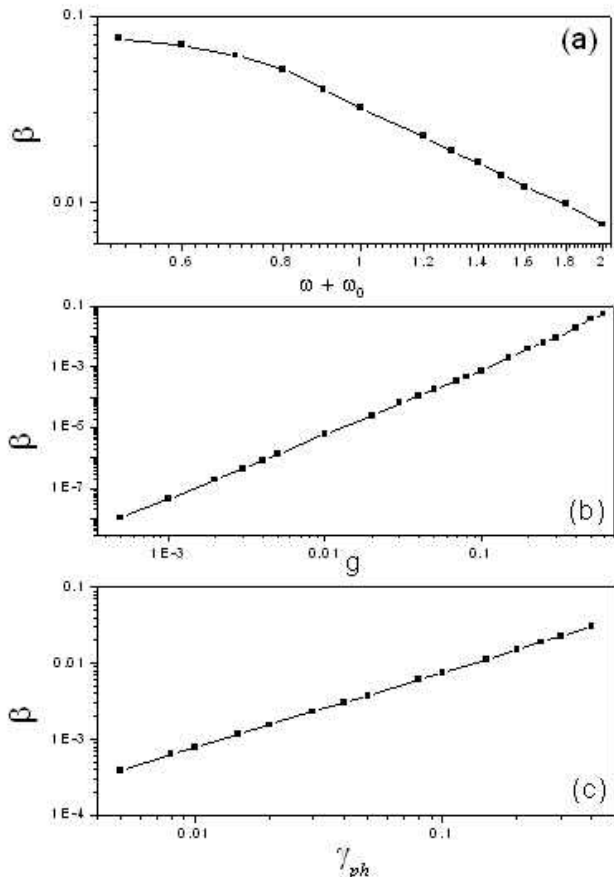


FIG. 3: Asymptotic photons generation rate $\beta \equiv d\langle n(\tau) \rangle / d\tau|_{\tau \rightarrow \infty}$ as function of **a)** $(\omega + \omega_0)$ for fixed g e γ_{ph} ; **b)** g for fixed γ_{ph} and ω_0 ; **c)** γ_{ph} for fixed g and ω_0 . We observe that $\beta \sim \gamma_{ph}$ and is inversely proportional to $\omega_0 + \omega$. In the weak coupling regime $\beta \sim g^2$.

doing this we eliminate the weight factors \sqrt{n} and $\sqrt{n+1}$ from the RH, since $E_+ |n\rangle = |n+1\rangle$ and $E_- |n\rangle = (1 - \delta_{n0}) |n-1\rangle$. In Fig. 2e we plot $\langle n \rangle$ for RH (line 1) and $\langle n_E \rangle$ obtained using H_E (line 2) *versus* τ for initial state $|\phi\rangle = |g, 0\rangle$. In both the cases there is photon creation from vacuum, although $\langle n_E \rangle$ increases slower than $\langle n \rangle$. Therefore this photon creation phenomenon is not due to the different weights \sqrt{n} and $\sqrt{n+1}$ attributed to the operators a and a^\dagger , but to the presence of the EM vacuum state.

From Fig. 1 we notice that asymptotically $\langle n(\tau) \rangle$ increases linearly with time, so one may gain a deeper insight into the problem by analyzing how the asymptotic photons generation rate $\beta \equiv d\langle n(\tau) \rangle / d\tau|_{\tau \rightarrow \infty}$ scales with $\omega + \omega_0$, g , and γ_{ph} (here we fix ω and vary other parameters). In Fig. 3a we plot β *versus* $(\omega + \omega_0)$ for fixed g e γ_{ph} , where we see that β increases when ω_0 decreases, so β is inversely proportional to $(\omega + \omega_0)$. Fig 3b shows the dependence of β on g for fixed γ_{ph} and ω_0 : for $g \ll 1$, the *weak coupling regime*, the analysis of the curve shows

that $\beta \sim g^2$, however such a dependence is modified for large values of g . Finally, Fig.3c shows that $\beta \sim \gamma_{ph}$ for fixed g and ω_0 , in agreement with the quantum trajectories approach: indeed, larger γ_{ph} implies larger jump probability and, consequently, in average $\langle n \rangle$ increases faster with time. A quantitative analysis of β will be presented elsewhere.

III. RANDOM FREQUENCY FLUCTUATIONS

One of the origins of dephasing from the physical point of view are the random shifts of the atomic transition frequency ω_0 due to the interaction with the environment [49, 54]. Indeed, $1/f$ noise in the bias controlling the atomic transition frequency is the dominant source of decoherence in superconducting artificial atoms (qubits) [32, 55, 56, 57]. To investigate the effect of such a noise on the dynamics of the atom-cavity system, we integrated numerically the master equation for the RH (neglecting the damping and dephasing) assuming that ω_0 has stochastic fluctuations. Our goal is to show that, when averaged over ensemble, this source of decoherence does asymptotically generate photons from vacuum, since its mathematical description is given by the dephasing Lindblad superoperator in the master equation we studied above.

As a simple model we considered time-dependent $\omega_0(t)$

$$\omega_0(t + dt) = \omega_0(t) + \begin{cases} 0.1\epsilon x r & \text{if } \omega_0(t) < \Omega_0 - 0.8\epsilon \\ -0.1\epsilon x r & \text{if } \omega_0(t) > \Omega_0 + 0.8\epsilon \\ 0.1\epsilon x (r - 1/2) & \text{otherwise} \end{cases}, \quad (7)$$

where $\Omega_0 \equiv \omega_0(t=0)$ is the mean atomic transition frequency, $r \in (-1, 1)$ is a random number, $\epsilon \ll 1$ is the maximum shift of the atom frequency and dt is the simulation unit step, $g dt \ll 1$. Here x is related to the ‘frequency’ of the noise: qualitatively, for $x \ll 1$ we have ‘low frequency’ noise, and in the opposite limit we have ‘high frequency’ noise.

We assumed the initial state $|g, 0\rangle$ and calculated the ensemble average of the mean photon number $\langle n \rangle_{av}$ and the probability of exciting the atom P_e using the parameters $\Omega_0 = 1$, $g = 6 \cdot 10^{-2}$, $\epsilon = g$. We considered three examples of noise whose spectra are shown in Fig. 4a: $x = 1$ corresponds to the ‘low frequency’ noise (line 1) and $x = 6$ is our reference to the ‘high frequency’ noise (line 3), while $x = 3$ is a case in between we call ‘middle frequency’ noise (line 2, data not shown in Fig. 1a since it lies between lines 1 and 3). First, the Fig. 4b shows three samples of $\langle n \rangle$ obtained for single runs of simulation for the ‘high frequency’ noise – one may see random rises and falls of photon number, however in average $\langle n \rangle$ increases. The Figs. 4c and 4d show $\langle n \rangle_{av}$ and P_e , respectively, obtained after averaging out many runs of simulations for the three kinds of noise. We see that in average there is a growth of both $\langle n \rangle_{av}$ and P_e ; moreover, the growth of $\langle n \rangle_{av}$ is approximately linear in time,

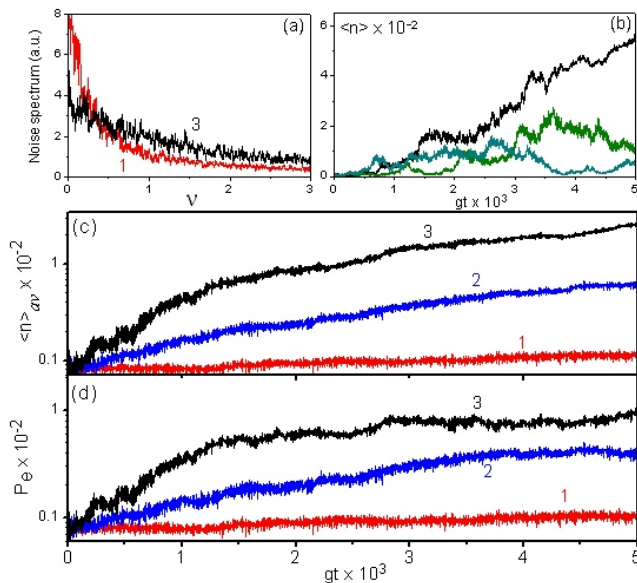


FIG. 4: Simulation of atomic dephasing via random atomic frequency fluctuations for parameters $\Omega_0 = 1$, $g = 6 \cdot 10^{-2}$, $\varepsilon = g$. **a**) Spectrum of the frequency noise $\omega_0(t) - \Omega_0$. Line 1 (red) corresponds to the ‘low-’ and line 3 (black) – to the ‘high-’ frequency noises. **b**) $\langle n \rangle$ for three individual runs of simulation using high frequency noise. **c**) $\langle n \rangle_{av}$ averaged out over many runs of simulation, showing photons growth, dependent on the noise frequency. Here line 2 (blue) is the ‘middle-frequency’ noise. **d**) P_e averaged out over many simulations. These curves agree qualitatively with the results obtained above using the master equation approach.

in agreement with our previous results.

From Fig. 4c we see that the photon generation rate is higher for higher frequency noise. One may understand qualitatively such a behavior as follows. The dynamics of the RH with externally prescribed non-random $\omega_0(t)$ allows for the coherent generation of both EM and atomic *real* excitations from vacuum for, e.g., periodic [44, 46, 47, 48] or linear [41, 43] time-dependence of $\omega_0(t)$. Moreover, the photon creation rate strongly depends on the shape of $\omega_0(t)$ [41] and, in the periodic case, on the periodicity of the modulation of $\omega_0(t)$ [44, 46]. The Fourier transform (Fig. 4a) of the noise contains the ‘resonant’ frequencies ($\nu \sim 2$ [44, 46]), with respective weights, for which photon generation occurs in the periodic case, so in average one expects a slow *incoherent* photon creation from vacuum due to these components in the noise spectrum. For the high frequency noise there are more resonant frequencies in the noise spectrum and/or their weight is larger compared to the low-frequency noise, so the photon growth rate is higher, in agreement with Fig. 4c.

Therefore, one of the physical origins of the photon creation through decoherence in cavity QED are the random fluctuations of the atomic transition frequency giving rise to effective time-dependent RH, for which pho-

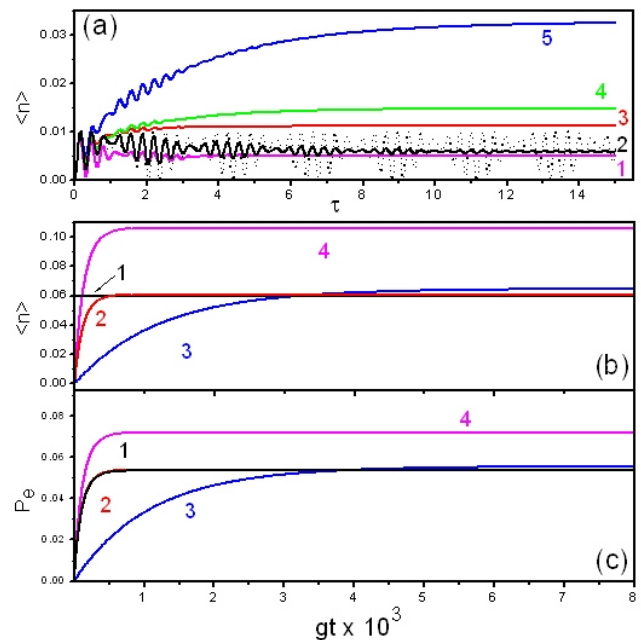


FIG. 5: **a**) $\langle n \rangle$ versus τ using the master equation (2) for initial state $|g, 0\rangle$ with parameters $\Delta = 0$, $g = 0.1$, $n_t = 0$ and decay rates $(\gamma_{ph}, \gamma, \kappa)$. Dotted line: $(0, 0, 0)$, line 1: $(0, 0, 1) \cdot 10^{-1}$, line 2: $(0, 1, 0) \cdot 10^{-1}$, line 3: $(1, 1, 1) \cdot 10^{-1}$, line 4: $(1, 0, 1) \cdot 10^{-1}$, line 5: $(1, 1, 0) \cdot 10^{-1}$. **b**) $\langle n \rangle$ versus gt for initial state $|g, 0\rangle$ using circuit QED parameters $\Delta = 0$, $g = 2 \cdot 10^{-2}$, $n_t = 6 \cdot 10^{-2}$ and distinct decay rates (line 1 denotes the thermal photon number n_t). Line 2: current parameters $(2, 3, 0.4) \cdot 10^{-4}$. Line 3: expected future scenario $(2, 3, 0.4) \cdot 10^{-5}$. Line 4: highly biased noise $(200, 3, 0.4) \cdot 10^{-4}$. For current parameters there is no observable difference between n_t and $\langle n \rangle$, however in the future or in very noisy environments $\langle n \rangle$ may become significantly larger than n_t due to photon creation through decoherence. **c**) P_e corresponding to the parameters in (b); P_e resembles the behavior of $\langle n \rangle$.

tons are created from vacuum for the ‘resonant’ frequencies [44, 46] present in the noise spectrum.

IV. DEPHASING PLUS RELAXATION

In realistic situations, besides the dephasing reservoir there are other important error sources (environments) acting on the system, e.g., thermal reservoirs. When other reservoirs are present, there is a competition between photon creation due to the atomic dephasing and photon losses due to the damping. In order to see this effect, we plot in Fig. 5a $\langle n \rangle$ versus τ for different decay rates in Eq. (2), for the parameters $\Delta = 0$, $g = 0.1$, $n_t = 0$ and the initial state $|g, 0\rangle$. The effect of temperature ($n_t > 0$) is just to shift the curves upward. The dotted line shows $\langle n \rangle$ in absence of any reservoir. When the atomic phase reservoir is switched off, the curve 1 with dissipation parameters $(0, 0, 1) \cdot 10^{-1}$ [we use nota-

tion $(\gamma_{ph}, \gamma, \kappa)$ and 2 with $(0, 1, 0) \cdot 10^{-1}$ show that for large times $\langle n \rangle$ is smaller than in the cases where the phase reservoir is switched on, as shown in the curves 3 with $(1, 1, 1) \cdot 10^{-1}$, 4 with $(1, 0, 1) \cdot 10^{-1}$ and 5 with $(1, 1, 0) \cdot 10^{-1}$. Even in situations in which the environment starts at $T = 0K$, in the asymptotic limit the system behaves as being subjected to an effective reservoir with $\tilde{n}_t > 0$, since $\lim_{\tau \rightarrow \infty} \langle n(\tau) \rangle > 0$. The number of effective reservoir photons \tilde{n}_t increases when the atomic phase reservoir is present (see curves 3, 4, and 5) and decreases when the atomic and field thermal reservoirs are predominant. However, the effective reservoir cannot be compared to the usual thermal reservoir, since the statistics of created field state is quite different from the thermal state statistics. A similar conclusion was drawn in [35], where the authors considered the master equation (2) at zero temperature with $\gamma_{ph} = \gamma = 0$, $\kappa \neq 0$ and showed that the antirotating part of the RH gives rise to a thermal-like term in the effective master equation, although it cannot be interpreted as an interaction with a thermal bath at a certain temperature.

In fig. 5b we consider current experimental parameters taken from recent circuit QED experiments [58] $\Delta = 0$, $g = 2 \cdot 10^{-2}$, $n_t = 6 \cdot 10^{-2}$. The line 1 shows the thermal photon number n_t and the line 2 shows $\langle n \rangle$ obtained via master equation (2) for current dissipation rates: $\kappa = 4 \cdot 10^{-5}$, $\gamma = 3 \cdot 10^{-4}$, $\gamma_{ph} = 2 \cdot 10^{-4}$. There is no visible deviation of $\langle n \rangle$ from n_t for the current temperatures, even if the detuning is increased to $\Delta = -0.2$ (data not shown). Next we consider the scenario expected in the future, where the damping losses are suppressed one order of magnitude, $\kappa = 4 \cdot 10^{-6}$, $\gamma = 3 \cdot 10^{-5}$, but the dephasing rate remains the same, $\gamma_{ph} = 2 \cdot 10^{-4}$. In this case (line 3), $\langle n \rangle$ slightly deviates from the thermal photon number n_t and such an effect could be observed in very accurate measurements. Finally, we take the current values of damping rates, $\kappa = 4 \cdot 10^{-5}$, $\gamma = 3 \cdot 10^{-4}$, and consider a highly biased noise [57] with the dephasing rate two order of magnitudes larger than the best one available today, $\gamma_{ph} = 2 \cdot 10^{-2}$ (line 4). In this case, $\langle n \rangle$ equals almost twice the thermal photons number due to the phenomenon of photon creation through decoherence.

Finally, in Fig. 5c we plot P_e corresponding to the parameters of Fig. 5b, where the line 1 shows P_e^{RWA} obtained for current dissipation parameters using RWA, which nearly does not depend on the relaxation rates. The behavior of P_e resembles the one of $\langle n \rangle$ and indicates that P_e increases due to the combined action of dephasing and the antirotating term, although for current parameters this phenomenon is insignificant. However, for a large γ_{ph} (line 4) P_e is substantially higher than P_e^{RWA} , demonstrating that large dephasing, besides decoherence, may also induce bit flip error.

V. DISCUSSION AND CONCLUDING REMARKS

We studied numerically the dynamics of the Rabi Hamiltonian subjected to dissipative losses, assuming *ad hoc* that one may describe the dissipative dynamics of the RH by using the standard master equation with usual damping and dephasing Lindblad superoperators. We found out that the atomic dephasing, when combined with the antirotating term in the RH, induces photon creation from vacuum. The physical interpretation of the phenomenon was given using two alternative approaches: 1) the quantum trajectories approach based on quantum jumps and 2) microscopic *ad hoc* model of dephasing based on stochastic oscillations of the atomic transition frequency (as occurs in solid state cavity QED). We showed that the photon creation through atomic decoherence is suppressed in the presence of damping mechanisms, and estimated the magnitude of this phenomenon using current experimental values of parameters, noting that the phenomenon might become relevant in future experiments.

We *do not* have a formal proof that the master equation (2) we used throughout this work is valid for the Rabi Hamiltonian in the strong atom-cavity coupling regime, since we assumed the Lindbladian dissipative superoperators without a microscopic deduction of the master equation. Nevertheless, the results obtained here are relevant for two reasons. First, if the master equation (2) is indeed applicable, it says that decoherence induces photons generation from vacuum, and such an effect may become relevant in future experiments with lower temperatures and lower damping rates. Second, if the master equation (2) turns out to be non-applicable to this problem, it will call attention that there is an incompatibility between the standard Lindbladian superoperators and antirotating terms in the Rabi Hamiltonians. In any case, more investigation of the problem is needed, since up to now the theoretical and numerical investigations were mainly concerned about the role of the RH antirotating term in the closed system dynamics, while our study points out novel important effects of the antirotating term in open systems.

Acknowledgments

The authors would like to thank the Brazilian agencies CNPq (T.W. and C.J.V-B), FAPESP #04/13705-3 (AVD), and UFABC (EID). This work was supported by Brazilian Millennium Institute for Quantum Information and FAPESP #2005/04105-5.

[1] I. I. Rabi, Phys. Rev. **49**, 324 (1926); **51**, 652 (1937).
 [2] C. Emary, Int. J. Mod. Phys. B. **17**, 5477 (2003).

[3] R. F. Bishop and C. Emary, J. Phys. A: Math. and General **34**, 5635 (2001).

- [4] R. F. Bishop, *et al.*, Phys. Lett. A **254**, 215 (1999); Phys. Rev. A **54**, R4657 (1996).
- [5] V. Fessatidis, J. D. Mancini, and S. P. Bowen, Phys. Lett. A **297**, 100 (2002).
- [6] A. Pereverzev and E. R. Bittner, Physical Chemistry Chemical Physics **8**, 1378 (2006).
- [7] N. Debergh and AB Klimov, Int. J. Mod. Phys. A **16**, 4057 (2001).
- [8] E. K. Irish, Phys. Rev. Lett. **99**, 173601 (2007).
- [9] H. G. Reik and M. Doucha, Phys. Rev. Lett. **57**, 787 (1986); H. Reik, *et al.* J. Phys. A **20**, 6327 (1987).
- [10] M. O. Scully and M. S. Zubairy, Quantum Optics, Cambridge University Press, 1997.
- [11] W. P. Schleich, Quantum Optics in Phase Space, WILEY-VCH Verlag, Berlin, 2001.
- [12] E. T. Jaynes and F. W. Cummings, Proc. IEEE **51**, 89 (1963).
- [13] B. W. Shore and P. L. Knight, J. Mod. Opt. **40**, 1195 (1993).
- [14] H. Mabuchi and A. C. Doherty, Science **298**, 1372 (2002).
- [15] J. M. Raimond, M. Brune, and S. Haroche, Rev. Mod. Phys. **73**, 565 (2001).
- [16] G. Rempe and H. Walther, Phys. Rev. Lett. **58**, 353 (1987).
- [17] M. Brune, *et al.*, Phys. Rev. Lett. **76**, 1800 (1996).
- [18] J. R. Kuklinski and J. L. Madaajczyk, Phys. Rev. A **37**, 3175 (1988);
- [19] M. Brune, *et al.*, Phys. Rev. A **45**, 5193 (1992).
- [20] M. Weidinger, B. T. H. Varcoe, R. Heerlein, and H. Walther, Phys. Rev. Lett. **82**, 3795 (1999).
- [21] S. J. D. Phoenix, and P. L. Knight, Phys. Rev. A **44**, 6023 (1991); Muhammed Yönaç, Ting Yu and J. H. Eberly, J. Phys. B: At. Mol. Opt. Phys. **39**, S621-S625 (1996).
- [22] J. I. Cirac and P. Zoller, Phys. Rev. Lett. **74**, 4091 (1995).
- [23] T. Pellizzari, S. A. Gardiner, J. I. Cirac, and P. Zoller, Phys. Rev. Lett. **75**, 3788 (1995); T. Sleator and H. Weinfurter, Phys. Rev. Lett. **74**, 4087 (1995).
- [24] S-B. Zheng and G-C. Guo, Phys. Rev. Lett. **85**, 2392 (2000); M.D. Barrett, *et. al.*, Nature **429**, 737 (2004).
- [25] M. A. Nielsen and I. L. Chuang, Quantum Computation and Quantum Information, Cambridge University Press, 2000.
- [26] I. Chiorescu *et al.*, Nature **431**, 159 (2004).
- [27] A. Wallraff *et al.*, Nature **431**, 162 (2004).
- [28] J. Johansson *et al.*, Phys. Rev. Lett. **96**, 127006 (2006).
- [29] A. Zagoskin and A. Blais, Physics in Canada **63**, 215 (2007).
- [30] J. P. Reithmaier *et al.*, Nature **432**, 197 (2004).
- [31] T. Yoshie *et al.*, Nature **432**, 200 (2004).
- [32] A. Blais *et al.*, Phys. Rev. A **69**, 062320 (2004).
- [33] A. Blais *et al.*, Phys. Rev. A **75**, 032329 (2007).
- [34] C. Gerry and P. Knight, Introductory Quantum Optics, Cambridge University Press, 2005.
- [35] A. B. Klimov, J. L. Romero, and C. Saavedra, Phys. Rev. A **64**, 063802 (2001).
- [36] J. Larson, Phys. Scr. **76**, 146 (2007).
- [37] G. Berlin and J. Aliaga, J. Opt. B: Quant. Semiclass. Opt. **6**, 231 (2004).
- [38] L. Bonci, R. Roncaglia, B. J. West, and P. Grigolini, Phys. Rev. Lett. **67**, 2593 (1991).
- [39] C. Emary and T. Brandes, Phys. Rev. Lett. **90**, 044101 (2003).
- [40] C. Emary and T. Brandes, Phys. Rev. E **67**, 066203 (2003).
- [41] K. Saito *et al.*, Europhys. Lett. **76**, 22 (2006).
- [42] K. Saito, M. Wubs, S. Kohler, Y. Kayanuma, and P. Hänggi, Phys. Rev. B **75**, 214308 (2007).
- [43] M. Wubs M, S. Kohler S, and P. Hanggi, Physica E - Low-Dimensional Systems and Nanostructures **40**, 187 (2007).
- [44] A. V. Dodonov, *et al.*, unpublished.
- [45] V. V. Dodonov, Modern Nonlinear Optics, second ed, volume **119**, 309 (2001).
- [46] C. Ciuti and I. Carusotto, J. Appl. Phys. **101**, 081709 (2007).
- [47] S. De Liberato, C. Ciuti, and I. Carusotto, Phys. Rev. Lett. **98**, 103602 (2007).
- [48] C. Ciuti, G. Bastard, and I. Carusotto, Phys. Rev. B **72**, 115303 (2005).
- [49] H. Carmichael, An open system approach to quantum optics, Springer-Verlag, 1993.
- [50] M. B. Plenio and P. L. Knight, Rev. Mod. Phys. **70**, 101 (1998) .
- [51] H. Goto and K. Ichimura, Phys. Rev. A **72**, 054301 (2005).
- [52] F. London, Z. Phys. **37**, 915 (1926); **40**, 193 (1927).
- [53] L. Susskind and J. Glogower, Physics **1**, 49 (1964).
- [54] Yu. Makhlin, G. Schön, and A. Shnirman, Rev. Mod. Phys. **73**, 357 (2001).
- [55] G. Ithier *et al.*, Phys. Rev. B **72**, 134519 (2005).
- [56] P. J. Leek *et al.*, Science **318**, 1889 (2007).
- [57] P. Aliferis, *et al.*, preprint at arXiv: 0806.0383.
- [58] D. I. Schuster *et al.*, Nature **445**, 515 (2007).